Physica E 41 (2009) 1169–1173

Contents lists available at ScienceDirect

Physica E

journal homepage: www.elsevier.com/locate/physe

Electron field emission properties of a gated conductive nanowire

Da Lei [a,b], Weibiao Wang [a,*], Leyong Zeng [a,b], Jingqiu Liang [c]

[a] Laboratory of Excited-State Processes, Changchun Institute of Optics, Fine Mechanics and Physics, Chinese Academy of Sciences, Changchun 130033, China
[b] Graduate School of Chinese Academy of Sciences, Beijing 100039, China
[c] State Key Laboratory of Applied Optics, Changchun Institute of Optics, Fine Mechanics and Physics, Chinese Academy of Sciences, Changchun 130033, China

ARTICLE INFO

Article history:
Received 25 April 2008
Accepted 8 January 2009
Available online 12 February 2009

PACS:
73.63.Fg
79.70.+q
73.40.Gk

Keywords:
Gated nanowire
Field emission
Enhancement factor

ABSTRACT

A gated nanowire model was proposed to estimate the field-emission performance of a conductive nanowire in gated structure. The actual electric fields around the nanowire top and the field-enhancement factor were calculated analytically based on an electrostatic theory. The influence of the device parameters such as the gate and anode voltages, the gate-hole radius, and the radius and length of the nanowire on the field-enhancement factor, the current and apex current density were discussed in detail. The results show that the field enhancement increases rapidly with the decrease of the gate-hole and nanowire radius, but the former almost increases linearly with the nanowire length. In addition, it was found that the current and current density at the edge of the nanowire increases exponentially with the gate and anode voltages.

© 2009 Elsevier B.V. All rights reserved.

1. Introduction

The nanowires such as carbon nanotubes, ZnO nanowires, and AuPd nanopillars have been considered as one kind of the best electron-emitting materials for vacuum microelectronic devices due to their remarkable field-emission properties [1–5]. Their excellent structure, unique mechanical, and electrical properties lead to the enhancement of the electric field on the top of the nanowires. The emission electrons can penetrate through the potential barrier into the vacuum through the tunneling effect [6,7], and a high current density appears at low electric field. Arrays of vertically aligned nanowires have been grown within patterned areas [8–10]. These field-emission cold cathodes are suitable for optoelectronic applications such as flat-panel displays, field-emission electron sources, microwave power amplifiers, etc [11–13].

Recently, the preparation of gated structures and triodes using nanopillars or CNT's act as emitters for devices were reported [14–19]. A number of field emitters with a closed hemispherical or hemielliptic top have been modeled [20–23] to obtain the potential distribution. Studies have shown that many parameters, including the aspect ratio of emitters, the intertube distance, the gate-hole radius, the gate–anode distance and the gate voltage, etc. can influence the field-emission properties of the nanowires [24–31]. Although the computer simulation and numerical calculation methods (for solving Laplace's equation) were successful in calculating the field distribution in various cases, there is a need for model systems, which can be solved analytically, from which the variation of the enhancement factor and emission current for various parameters can be easily determined.

In our previous work [32], the field-enhancement factor of the gated open nanotube was studied in the case of the nanotube height being equal to the gate–cathode distance. To broadly understand the field-emission properties of the gated nanowires, a model of gated single-conductive nanowire with a flat circular top that protrudes through the gate circular hole was proposed in this paper. The actual fields around the top of the gated nanowire, field-enhancement factor, and emission current from the nanowire were calculated by an electrostatic theory. These obtained fields and potential distribution are in agreement with the results of computer and numerical simulation [29–31]. The effect of the parameters of the device on the field-enhancement factor, the emission current, and apex current density were investigated.

2. Model

The two infinite parallel flat planes at horizontal direction with the spacing of d_1 were taken as the gate and cathode electrodes, respectively. The gate plane had only one circular gate hole with the radius R (in micrometers scale). The conductive nanowire with a radius r_0 and a height L (a few micrometers) was operated as the electron emitter of device and the nanowire top surface was

* Corresponding author.
E-mail address: wangwbt@126.com (W. Wang).

1386-9477/$ - see front matter © 2009 Elsevier B.V. All rights reserved.
doi:10.1016/j.physe.2009.01.017

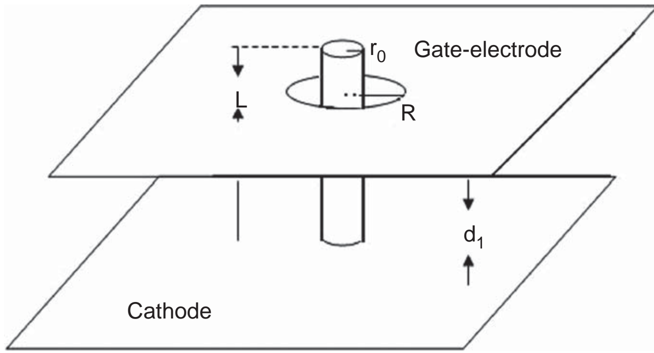

Fig. 1. Geometric model of the gated nanowire.

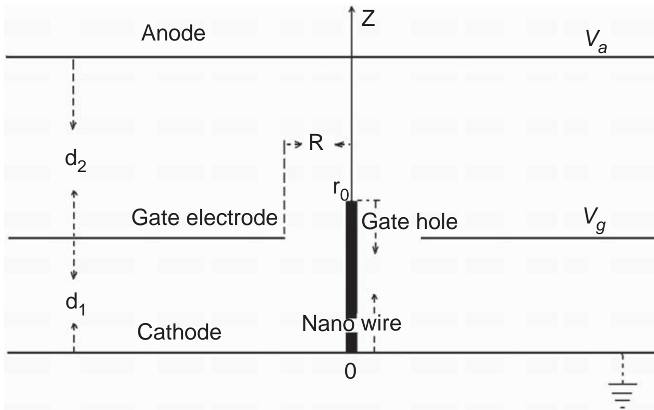

Fig. 2. Calculation model of the gated nanowire.

considered as a flat plane. The conductive nanowire was vertically stood on the cathode plane and protrudes through the center of the circular gate hole as shown in Fig. 1.

To compute the actual fields near the nanowire, we assumed that the cathode potential was zero and the potential on all the surface of the nanowire was kept equal to the cathode potential. An additional anode electrode was introduced over the gate electrode with a space of d_2 to the gate plane and parallel with the gate electrode as shown in Fig. 2. To simplify the situation, the anode and gate potentials were considered as V_a and V_g, and the space-charge effects, the thickness of the gate electrode, and the Coulomb interactions between the edge of the infinite electrodes and the nanowire were neglected in this study.

3. Field calculation around the gated nanowire

3.1. Theory

The cylindrical coordinate systems have been used in this calculation and the intersection point of the cathode electrode and the tube axis are taken as the origin as shown in Fig. 2. Since the space-charge effects can be ignored, the potential distribution near the nanowire in the gated structure satisfies Laplace's equation,

$$\nabla^2 \Phi(z, r, \varphi) = 0. \tag{1}$$

The boundary conditions are as follows: $\Phi|_{z=0} = 0$, $(\partial\Phi/\partial r)|_{z=(d_1+d_2)} = 0$, $\Phi|_{z=(d_1+d_2)} = V_a$, $\Phi|_{z=d_1}^{r\geqslant R} = V_g$, and $\Phi|_{r=r_0} = 0$ in the region of $0\leqslant z\leqslant L$.

The solutions of Eq. (1) obtained through the separation of variables when $k=0$ and $k>0$, respectively, which can be expressed as

$$\Phi(z, r) = (az+b) \times (A \ln r + B) \quad (k=0), \tag{2}$$

$$\Phi(z, r) = [a' \exp(kz) + b' \exp(-kz)] \times [A' J_0(kr) + B' N_0(kr)] \quad (k>0), \tag{3}$$

where k, a, b, A, B, a', b', A', and B' are constants, $J_0(kr)$ and $N_0(kr)$ are Bessel and Neumann functions of order zero, respectively.

3.2. Electric field around the nanowire side

For Eqs. (2) and (3) above, the function $\Phi(z, r)$ must be a finite value because the potential is finite in our model, however, the term In(r) in Eq. (2) has been limited as $\lim_{r\to\infty} \ln(r) \to \infty$ or $\lim_{r\to 0} \ln(r) \to -\infty$ if r tends to be infinite or zero, and the potentials are zero on the surfaces of nanowire and cathode. Hence, the solution in Eq. (2) cannot exist, the electric potential near the nanowire is only determined by Eq. (3) in the region of $0\leqslant z\leqslant L$. Considering the boundary conditions $\Phi|_{z=0} = 0$ and $\Phi|_{r=r_0} = 0$, the electric potential distribution near the nanowire can be expressed by

$$\Phi(z, r) = \sum_{i=1}^{\infty} A''_i \times \left[J_0(k_i r) - \frac{J_0(k_i r_0)}{N_0(k_i r_0)} N_0(k_i r)\right] \times sh(k_i z), \tag{4}$$

where A''_i ($i = 1, 2, 3,\ldots$) are constants. On the other hand, the electric potential must be a solution of Laplace's Eq. (1), so Eq. (4) can be rewritten as

$$\Phi(z, r) = \Psi_1(z) \times \Psi_2(r), \tag{5}$$

where $\Psi_1(z)$ and $\Psi_2(r)$ are functions of z and r, respectively. From Eq. (3), we can see that the function $\Psi_2(r)$ can be expressed as a linear superposition of both Bessel $J_0(k'r)$ and Neumann $N_0(k'r)$ functions in the region of $k'>0$, i.e., $\Psi_2(r) = CJ_0(k'r)+DN_0(k'r)$ where k', C, and D are constants. Based on the boundary condition $\Phi|_{r=r_0} = 0$ the function above can be written as $\Psi_2(r) = C' \times [J_0(k'r) - J_0(k'r_0)N_0(k'r)/N_0(k'r_0)]$. Thus, the function $\Phi(L, r)$ can be expressed by

$$\Phi(L, r) = U_m \times [J_0(k'r) - J_0(k'r_0)N_0(k'r)/N_0(k'r_0)], \tag{6}$$

where C' and U_m are coefficients. If the constant k' assumed as $k' = k_1$, the following equations $A''_1 = U_m/sh(k_1 L)$, $A''_i = 0$ ($i = 2, 3, 4,\ldots$) are obtained from Eqs. (4) and (6) at $z = L$, and the electric potential near the nanowire can be expressed by

$$\Phi(z, r) = U_m \times \frac{sh(k_1 z)}{sh(k_1 L)} \times \left[J_0(k_1 r) - \frac{J_0(k_1 r_0) N_0(k_1 r)}{N_0(k_1 r_0)}\right]. \tag{7}$$

We select that the coefficient U_m is $V_g+(V_a-V_g)(L-d_1)/d_2$, thus the expression (7) can be rewritten as

$$\Phi(z, r) = \left[V_g + \frac{(V_a - V_g)}{d_2}(L - d_1)\right] \times \frac{sh(k_1 z)}{sh(k_1 L)} \times \left[J_0(k_1 r) - \frac{J_0(k_1 r_0) N_0(k_1 r)}{N_0(k_1 r_0)}\right]. \tag{8}$$

Considering the boundary condition $\Phi|_{z=d_1}^{r=R} = V_g$, we can obtain the following equation:

$$V_g = \left[V_g + \frac{(V_a - V_g)}{d_2}(L - d_1)\right] \times \frac{sh(k_1 d_1)}{sh(k_1 L)} \times \left[J_0(k_1 R) - \frac{J_0(k_1 r_0) N_0(k_1 R)}{N_0(k_1 r_0)}\right]. \tag{9}$$

The k_1 can be determined by Eq. (9).

Hence, the corresponding electric field intensities E_r and E_z in the radial and the axial directions are obtained

$$E_z = -k_1\left[V_g + \frac{(V_a - V_g)}{d_2}(L - d_1)\right] \times \frac{sh(k_1 z)}{sh(k_1 L)} \times \left[J_0(k_1 r) - \frac{J_0(k_1 r_0)N_0(k_1 r)}{N_0(k_1 r_0)}\right], \tag{10}$$

$$E_r = k_1\left[V_g + \frac{(V_a - V_g)}{d_2}(L - d_1)\right] \times \frac{sh(k_1 z)}{sh(k_1 L)} \times \left[J_1(k_1 r) - \frac{J_0(k_1 r_0)N_1(k_1 r)}{N_0(k_1 r_0)}\right]. \tag{11}$$

3.3. Electric fields over the nanowire top

Similarly, from the boundary conditions $(\partial\Phi/\partial r)|_{z=(d_1+d_2)} = 0$ and $\Phi|_{z=(d_1+d_2)} = V_a$ the potential over the nanowire top can be expressed as

$$\Phi(z,r) = V_g + (V_a - V_g)\frac{(z - d_1)}{d_2} + \sum_i B'_{k_i}\exp(-k_i z)\{1 - \exp[-2k_i(d_1 + d_2 - z)]\} \times J_0(k_i r), \tag{12}$$

where B'_{k_i} is constant.

We can assume that the third term in Eq. (12) as $U(z) \times J_0(k_1 r)$, and then considering the boundary condition (where the potentials are zero on the top surface of nanowire) the potential over the nanowire top can be approximately obtained in the region of $r \leqslant r_0$,

$$\Phi(z,r) = V_g + (V_a - V_g)\frac{(z - d_1)}{d_2} - \frac{[V_a(L - d_1) + V_g(d_1 + d_2 - L)]\{1 - \exp[-2k_1(d_1 + d_2 - z)]\}}{d_2\exp[k_1(z - L)]\{1 - \exp[-2k_1(d_1 + d_2 - L)\}}. \tag{13}$$

Thus, the corresponding electric-field intensities are

$$E_r = 0, \tag{14}$$

$$E_z = -\frac{(V_a - V_g)}{d_2} - k_1\frac{[V_a(L - d_1) + V_g(d_1 + d_2 - L)]\{1 + \exp[-2k_1(d_1 + d_2 - z)]\}}{d_2\exp[k_1(z - L)]\{1 - \exp[-2k_1(d_1 + d_2 - L)\}}. \tag{15}$$

4. Field enhancement factor and emission current

The field-enhancement factor β is defined as $\beta = E_a/E_m$, [32] where E_a is the actual electric field of the apex of nanowire and E_m is the macroscopic applied electric field. Further the macroscopic electric field between the anode and cathode in the diode structure can be expressed as $E_m = V_a/(d_1+d_2)$ that is considered as the macroscopic electric field in this study. Because of the cross section of the nanowire end is a flat plane, the actual field on the nanowire edge can be expressed by $E_a = \sqrt{E_z^2 + E_r^2}$. Thus, the field-enhancement factor obtained

$$\beta = \sqrt{\beta_1^2 + \beta_2^2}, \tag{16}$$

where $\beta_1 \approx 1 + k_1(L - d_1) + [k_1(d_1 + d_2 - L) - 1]V_g/V_a$, $\beta_2 \approx [(L - d_1) + (d_1 + d_2 - L)V_g/V_a]R(k_1 r_0)$, and $R(k_1 r_0) = k_1[J_1(k_1 r_0) - J_0(k_1 r_0)N_1(k_1 r_0)/N_0(k_1 r_0)]$, respectively.

Fowler–Nordheim equation was used to calculate the current densities of nanowire surfaces, i.e.,

$$J = 1.54 \times 10^{-6} \times \frac{E^2}{\phi t^2(y)}\exp\left(-8.3 \times 10^7 \times \frac{\phi^{3/2}u(y)}{E}\right), \tag{17}$$

where ϕ is the work function of the efficient emission area of the nanowire surfaces, E the actual electric field on the nanowire surface, and $t(y) = 1.1$, $y = 3.79 \times 10^{-4}E^{1/2}/\phi$, and $u(y) = 0.95 - y^2$, respectively [24].

The emission current I can be determined by the total emission current from the efficient emission area near the nanowire top edge on the outside of nanowire because the actual electric fields on the top surface and side region of $z < d_1$ of nanowire cannot produce the emission electrons from nanowire surfaces because the fields are not enough larger in this case. Thus, the emission current can be approximated by Eq. (18) based on the cylindrical model of nanowire

$$I \approx \int_{d_1}^{L} 2\pi r_0 J(E)\,dz, \tag{18}$$

where E is the function of z.

5. Results and discussions

The equipotential lines near the nanowire top in gated structure obtained by the computer simulation method are plotted in Fig. 3. We can see that the potential near the nanowire top increases rapidly with the increase of r and z, and the potential approach the fixed values when the distance from the outside the nanowire tends to be a larger value.

The electric fields and potentials near the nanowire side are calculated with the device parameters of $L = 9\,\mu m$, $R = 5\,\mu m$, $r_0 = 10\,nm$, $d_1 = 8\,\mu m$, $d_2 = 200\,\mu m$, $V_a = 2000\,V$ and $V_g = 50\,V$, and their dependence on r is shown in Fig. 4(a) and (b). The electric-field intensity around the nanowire decreases fleetly with the r and finally reaches a fixed value of about 9.35 V/μm. The variation rate of the electric-field intensity decreases with the increase of r and approaches zero. Along the r direction, the potential near the nanowire top increases from 0 to 62 V and then tends to about 59.7 V in the region of $5\,\mu m < r$. These results are in good agreement with the computer simulation results mentioned above.

Fig. 5 shows the field-enhancement factor β as a function of the gate-hole radius R when the device parameters are taken as $V_a = 2000\,V$, $V_g = 50\,V$, $d_1 = 8\,\mu m$, $d_2 = 200\,\mu m$, and $L = 9\,\mu m$ for the different nanowire radii of 10, 20, and 30 nm. The enhancement factor decreases rapidly with the increase of either r_0 or R

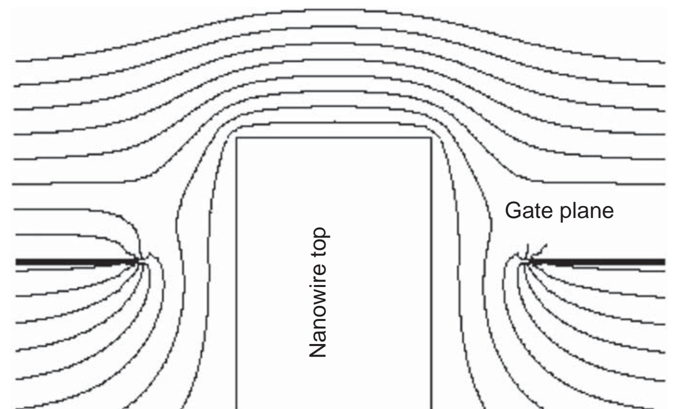

Fig. 3. Equipotential lines near the gated nanowire top.

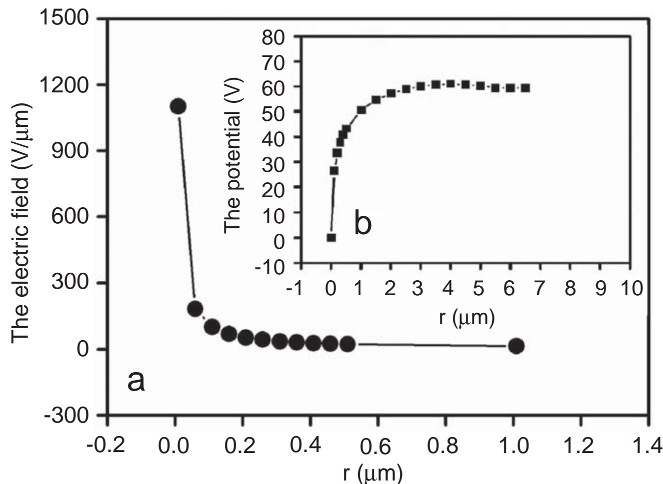

Fig. 4. Curves of the electric fields and potential distribution near the nanowire top outside at $L = 9\,\mu m$, $R = 5\,\mu m$, $r_0 = 10\,nm$, $d_1 = 8\,\mu m$, $d_2 = 200\,\mu m$, $V_a = 2000$ V, and $V_g = 50\,V$; (a) the curve of the electric field for r; (b) the curve of the potential vs. r.

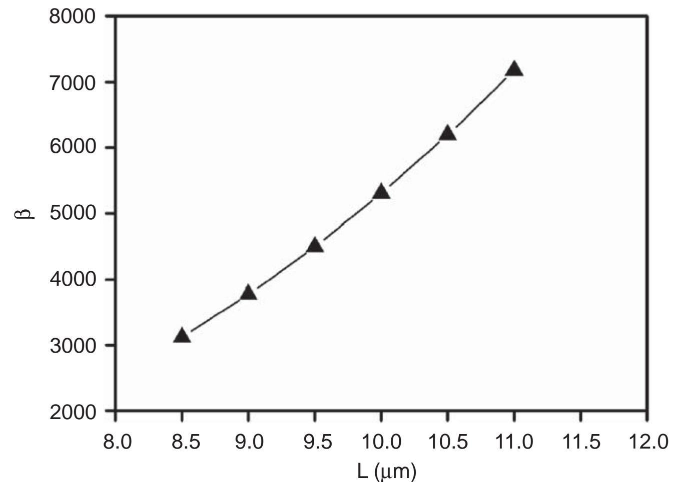

Fig. 6. Plot of the enhancement factor for nanowire length L when the parameters of $V_a = 2000\,V$, $V_g = 50\,V$, $d_1 = 8\,\mu m$, $d_2 = 200\,\mu m$, $r_0 = 20\,nm$, and $R = 3\,\mu m$.

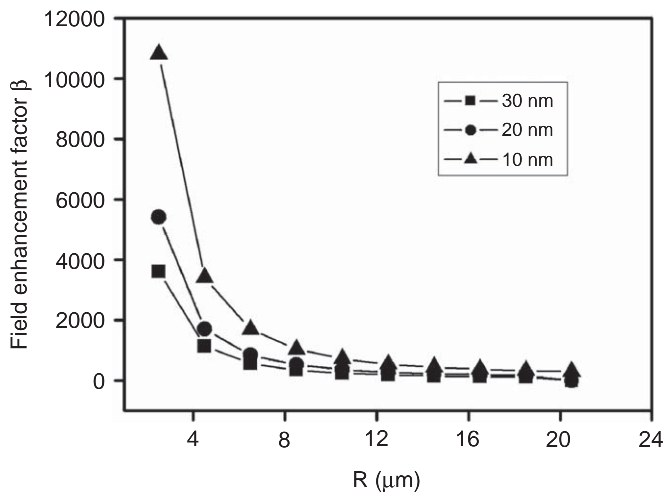

Fig. 5. Plots of the enhancement factor β vs. gate-hole radius when the device parameters of $V_a = 2000\,V$, $V_g = 50\,V$, $d_1 = 8\,\mu m$, $d_2 = 200\,\mu m$, $L = 9\,\mu m$, and different nanowire radii, i.e., 10, 20, and 30 nm, respectively. (For interpretation of the references to color in this figure legend, the reader is referred to the web version of this article.)

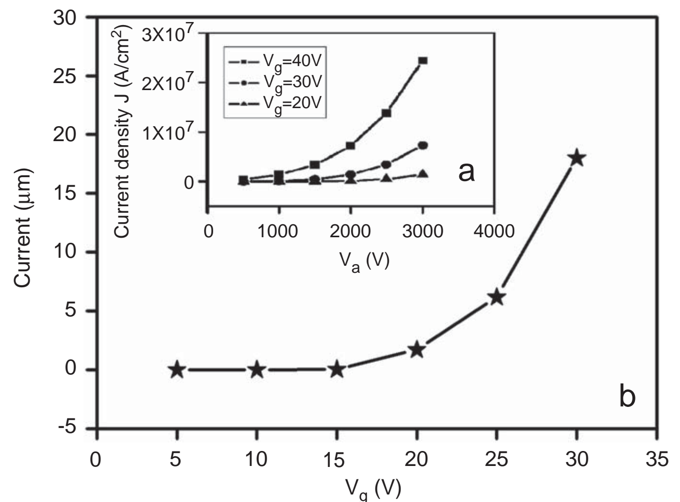

Fig. 7. Curves of the current and current density for gate or anode voltages at $L = 10\,\mu m$, $d_1 = 8\,\mu m$, $d_2 = 200\,\mu m$, $r_0 = 20\,nm$, and $R = 5\,\mu m$; (a) current density J as a function of the anode voltage V_a for the different gate voltages 20, 30, and 40 V; (b) plot of the total current vs. gate voltages at $V_a = 2000\,V$. (For interpretation of the references to color in this figure legend, the reader is referred to the web version of this article.)

and tends to be constant (i.e., about 10^2), which is equal to the aspect ratio of the individual nanowire with a few micrometers of length ($L = 9\,\mu m$) and a few ten nanometers radii (10–30 nm) when R becomes infinite.

The enhancement factor as a function of the nanowire length L when the device parameters are taken as $V_a = 2000\,V$, $V_g = 50\,V$, $d_1 = 8\,\mu m$, $d_2 = 200\,\mu m$, $r_0 = 20\,nm$, and $R = 3\,\mu m$ is shown in Fig. 6. The enhancement factor β increases almost linearly with the nanowire length L, and its slope is about 1720 (1 per micrometer) per micrometer.

To compute the current I from the apex of the gated nanowire, we assumed that the work function of the nanowire top surface is about 5 eV. The calculated results with the device parameters of $L = 10\,\mu m$, $d_1 = 8\,\mu m$, $d_2 = 200\,\mu m$, $r_0 = 20\,nm$, and $R = 5\,\mu m$ are shown in Fig. 7(a) and (b). Fig. 7(a) shows that the current density on the top edge of the nanowire increases greatly with increasing the gate voltage V_g, and exponentially with increasing the anode voltage V_a. Fig. 7(b) is the curve of emission current of the gated nanowire vs. the gate voltage at the anode voltage of 2000 V. The emission current increases from 3×10^{-6} to 18 μA when the gate voltage increases from 5 to 30 V, especially the slope of the curve becomes much large when $15\,V < V_g$, for example, the slope of the curve is around 0.0039 μA/V in the region of $5\,V \leqslant V_g \leqslant 15\,V$ and is about 1.63 μA/V in the region of $20\,V \leqslant V_g \leqslant 30\,V$.

6. Conclusions

A gated conductive nanowire model was proposed to obtain the actual electric field near the top of nanowire in this paper. The field-enhancement factors as a function of the geometrical parameters including the gate-hole radius, the nanowire radius, and the emitter height were discussed. The dependence of the total current and apex current density on the gate and anode voltages were also discussed. This work provides useful information for the fabrication and design of the gated nanowire cold cathode for field-emission display panels and other nanoscale gated structure of devices.

Acknowledgment

The authors gratefully acknowledge the financial support from the National Natural Science Foundation of China (Grant nos. 50072029 and 50572101).

References

[1] W.I. Milne, K.B.K. Teo, M. Chhowalla, G.A.J. Amaratunga, D. Pribat, P. Legagneux, G. Pirio, V.T. Binh, V. Semet, Curr. Appl. Phys. 2 (2002) 509.
[2] W. Zhua, C. Bower, O. Zhou, G. Kochanski, S. Jin, Appl. Phys. Lett. 75 (1999) 873.
[3] G. Pirio, P. Legagneux, D. Pribat, K.B.K. Teo, M. Chhowalla, G.A.J. Amaratunga, W.I. Milne, Nanotechnology 13 (2002) 1.
[4] W. Chen, H. Ahmed, J. Vac. Sci. Technol. B 11 (1993) 2519.
[5] W. Chen, H. Ahmed, K. Nakazato, Appl. Phys. Lett. 66 (1995) 3383.
[6] P.N. Minh, L.T.T. Tuyen, T. Ono, H. Miyashita, Y. Suzuki, H. Mimura, M. Esashi, J. Vac. Sci. Technol. B 21 (2003) 1705.
[7] J.H. Choi, S.H. Choi, J.H. Han, J.B. Yoo, C.Y. Park, T. Jung, S.G. Yu, I.T. Han, J.M. Kin, J. Appl. Phys. 94 (2003) 487.
[8] Q.D. Chen, L.M. Dai, J. Nanosci. Nanotech. 1 (2001) 43.
[9] X.P. Xu, G.R. Brandes, Appl. Phys. Lett. 74 (1999) 2549.
[10] Y.H. Lee, Y.T. Jang, D.H. Kim, J.H. Ahn, B.K. Ju, Adv. Mater. 13 (2001) 479.
[11] W.A.D. Heer, A. Chatelain, D. Ugarte, Science 270 (1995) 1179.
[12] P.G. Collins, A. Zettl, Phys. Rev. B 55 (1997) 9391.
[13] K.B.K. Teo, M. Chhowalla, G.A. Amaratunga, W.I. Milne, G. Pirio, P. Legagneux, D. Pribat, D.G. Hasko, Appl. Phys. Lett. 80 (2002) 2011.
[14] A.A.G. Driskill-Smith, D.G. Hasko, H. Ahmed, Appl. Phys. Lett. 75 (1999) 284.
[15] A.A.G. Driskill-Smith, D.G. Hasko, H. Ahmed, J. Vac. Sci. Technol. B 15 (1997) 2773.
[16] A.A.G. Driskill-Smith, D.G. Hasko, H. Ahmed, J. Vac. Sci. Technol. B71 (1997) 3159.
[17] D.S.Y. Hsu, Appl. Phys. Lett. 80 (2002) 2988.
[18] D.S.Y. Hsu, J. Shaw, Appl. Phys. Lett. 80 (2002) 118.
[19] K.H. Park, W.J. Seo, S. Lee, K.H. Koh, Appl. Phys. Lett. 81 (2002) 358.
[20] T. Asano, IEEE Trans. Electron Devices ED-38 (1991) 2392.
[21] D.W. Jenkins, IEEE Trans. Electron Devices ED-40 (1993) 666.
[22] E.G. Zaidman, IEEE Trans. Electron Devices ED-38 (1991) 2392.
[23] D. Nicolaescu, Appl. Surf. Sci. 76/77 (1994) 47.
[24] N. Shi, D.F. Pi, Proc. SPIE. 4600 (2001) 196.
[25] J.C. Shi, S.Z. Deng, N.S. Xu, R.H. Yao, J. Chen, Appl. Phys. Lett. 88 (2006) 013112.
[26] Y.C. Lan, C.T. Lee, Y. Hu, S.H. Chen, C.C. Lee, B.Y. Tsui, T.L. Lin, J. Vac. Sci. Technol. B 22 (2004) 1244.
[27] Y.M. Wong, W.P. Kang, J.L. Davidson, B.K. Choi, W. Hofmeister, J.H. Huang, Diamond Relat. Mater. 14 (2005) 2069.
[28] A.A.G. Driskill-Smith, D.G. Hasko, H. Ahmed, J. Vac. Sci. Technol. B 18 (2000) 3481.
[29] D. Nicolaescu, V. Filip, S. Kanemaru, J. Itoh, J. Vac. Sci. Technol. B 21 (2003) 366.
[30] D. Nicolaescu, J. Vac. Sci. Technol. B 13 (1995) 531.
[31] D. Nicolaescu, M. Nagao, V. Filip, S. Kanemara, J. Itoh, et al., Jpn. J. Appl. Phys. 44 (2005) 3854.
[32] D. Lei, L.Y. Zeng, W.B. Wang, J.Q. Liang, J. Appl. Phys. 102 (2007) 114503.